A Digital Morphometric Comparison of Nucleolar Features in BAP1-Mutant Versus BAP1-Wildtype Uveal Melanomas

Korina Steinbergs, MD[1,4], Ian Dryden, MD[1,4], Nandita Bhaskhar, PhD[2], Minhaj Alam, PhD[3], Jonathan Lin, MD PhD[1,4]

Departments of [1]Pathology, [2]Electrical Engineering, and [3]Biomedical Data Science, Stanford University, Stanford, CA [4]VA Palo Alto Health Care System, Palo Alto, CA

Background

Uveal melanomas (UM) are the most common primary intraocular malignancy in adults. Callender was the first to devise a histologic classification of UM in attempt to correlate morphologic features with prognosis in 1931[1]. In 1983, McClean et al found that nucleolar size, as measured by standard deviation of nucleolar area, was as an important prognostic feature in UM[2]. In 1989, Huntington et al were the first to describe a technique to measure the mean of the ten largest nucleoli (MTLN) in a 5 mm central linear strip that predicted mortality in UM[3]. In 1997, Mclean et al were the first to use automated image capture analysis (AICA) of the silver stain for nucleolar organizing regions (AgNOR) method to predict uveal melanoma patient outcomes[4]. In 2004, Onken et al used gene expression profiling (GEP) to prognostically categorize UMs as either Class 1 (low risk) or Class 2 (high risk) tumors[5]. In 2010, Harbour et al found that most high-risk metastatic UMs harbor a deactivating mutation BRCA1 associated protein-1 (BAP1) gene, a tumor suppressor gene located on chromosome 3p[6]. Recent image analysis investigations have shown that the digital morphometry of tumor nuclei correlate with BAP-1 status; however, the relationship between BAP1 status and nucleolar features remains to be described[7,8].

Methods

The BAP1 mutation status of 10 UMs was determined immunohistochemically with use of anti-BAP1 monoclonal antibody (C-4, Santa Cruz Biotechnology, sc-28383) and confirmed molecularly with use of a solid tumor actionable mutation panel.

Manual Method: 10 H&E stained slides composed of 5 BAP1-mutant and 5 BAP1-wildtype UMs were scanned via Philips IntelliSite Scanner and uploaded as whole slide images to the Phillips Intellisite Suite for morphometric analysis. The longest nucleolar diameter (in µm) and the number of nucleolar organizing regions (NORs) was determined for a two hundred consecutive tumor nuclei in one high-powered field in each slide for a total of 2,000 tumor cells (Figure 1A). A paired two-sample t-test was performed to determine if a statistical difference existed between the mean longest nucleolar diameter and the NOR number in the BAP1-mutant (Figure 1B) versus BAP1-wildtype groups (Figure 1C).

Automated Method: 10 whole slide images of 5 BAP1-mutant and 5 BAP1-wildtype UMs were extracted as high resolution PNG image files (Figure 2A). Each image was split into fixed-size (224 x 224 px) patches for cell segmentation (Figure 2B, 2C). The Cellpose algorithm, a deep learning-based segmentation method, was used for nuclear segmentation[9,10,11]. A nuclei segmentation model from Cellpose was applied to inverted grayscale images of the patches to get nucleus segmentation masks (Figure 2D). To reduce spurious features, the masks were preprocessed by removing the mask edges to eliminate partial nuclei, fill holes, and small masks < 30 px (Figure 2E). Each nuclear mask was extracted from its patch using a connected components algorithm and converted to a high contrast grey scale image (Figure 3). Isolated nuclear plots were processed using two different thresholding algorithms to identify NORs: 1) an adaptive method that set the threshold value to be the mean of a parameterized neighborhood area (chosen to be 11) minus a constant (chosen to be 2), and 2) a customized method that set the threshold to the first quartile of the cumulative distribution of the normalized pixel histogram (Figure 3). The identified NORs were then processed to remove single pixel regions (noise) and an opening processing step (an erosion followed by a dilation) to remove small spots and connect cracks. The number of NORs were counted, and the pixel area of each NOR was calculated along with the nucleus pixel area. After using each thresholding technique, 3,887 nuclear plots for the BAP1-mutant group and 3,667 nuclear plots for the BAP1-wildtype group were obtained. Nuclear plots that did not contain a measurable NOR count and NORs that measured >100 and <10 pixel area, were excluded from the dataset, which yielded 2,129 nuclear plots for the statistical analysis. Statistical means were calculated for the NOR counts and maximum NOR pixel area for each method. A paired two sample t-test was performed to determine if a statistical difference existed between the BAP1-mutant versus BAP1-wildtype groups in terms of the largest NOR pixel area (nucleolus) and the number of NORs.

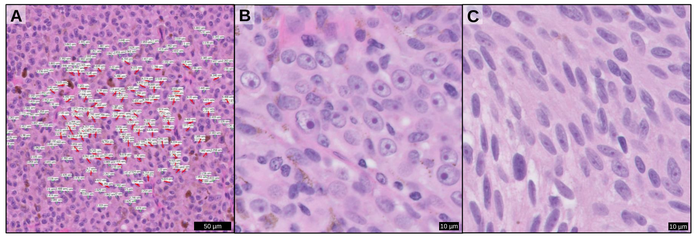

Figure 1: Digitally scanned H&E stained slides of uveal melanomas. A) Manual measurements of nuclei and nucleoli at a single high powered field (40x scanned objective). B) BAP1-mutant UM with prominent nucleoli and few nucleolar organizing regions (100x scanned objective). C) BAP1-wildtype UM with distinct nucleoli and more nucleolar organizing regions (100x scanned objective).

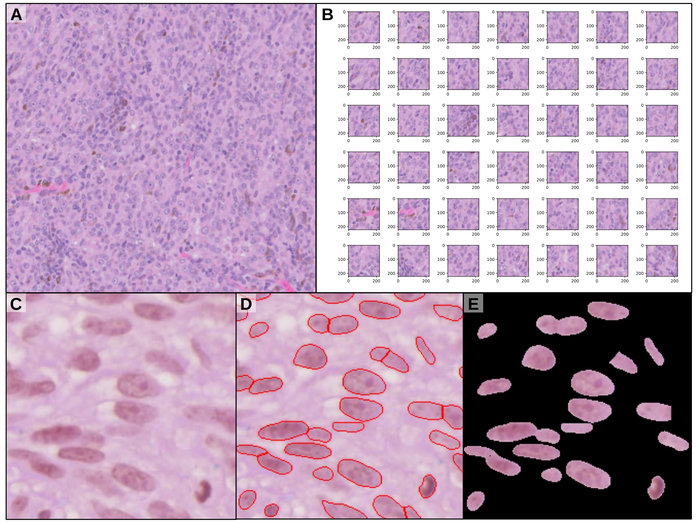

Figure 2: Image analysis of BAP1-mutant uveal melanomas. A) Extracted high resolution .png file from whole slide image. B) Extracted image split into 224 x 224 pixel sized patches. C) A single 224 x 224 pixel patch. D) Predicted cell segmentations masks (red) overlaid on a patch image. E) Processed nuclear segmentation masks.

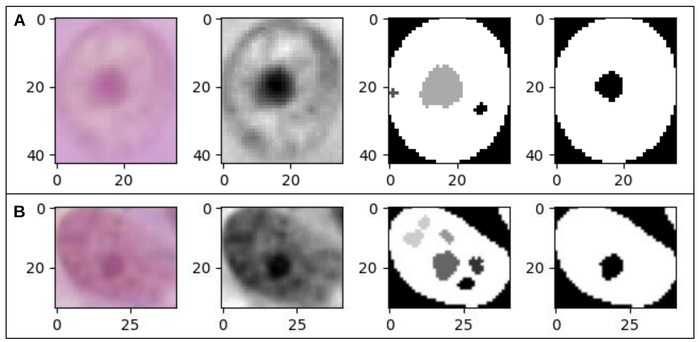

Figure 3: Representative image analysis plots of a UM nuclei and NORs in color (far left), high contrast grey scale (second to left), Adaptive Thresholding (second to right), and Custom Thresholding (far left). A) Adaptive Thresholding shows 3 NORs with a maximum pixel area of 121, while Custom Thresholding shows 1 NOR with a maximum pixel area of 52 in a BAP1-mutant UM. B) Adaptive Thresholding shows 6 NORs with maximum pixel area of 63, while Custom Thresholding shows 1 NOR with a maximum pixel area of 49 in a BAP1-wildtype UM.

Results

Manual Measurement Method: The BAP1-mutant group had a mean longest nucleolar diameter of 2.43 µm (range 1 - 9.1) and a mean NOR count of 1.4 (range 1 - 5). The BAP1-wildtype group had a mean longest nucleolar diameter of 2.15 µm (range 0.5 - 6) and a mean NOR count of 2 (range 1 - 6). A strong statistical difference between the mean longest nucleolar diameter ($P = 7.65E^{-24}$) and the mean NOR count ($P = 4.68E^{-47}$) was observed between BAP1-mutant and BAP1-wildtype groups.

Adaptive Thresholding Method: The BAP1-mutant group had a mean largest NOR pixel area of 52.3 (range 11 - 99) and a mean NOR count of 2.3 (range 1 - 11). The BAP1-wildtype group had a mean largest NOR pixel area of 47.75 (range 11 - 99) and a mean NOR count of 2.4 (range 1 - 12). A statistical difference between the mean largest NOR pixel area ($P = 1.0072E^{-09}$) was observed between the BAP1-mutant and BAP1-wildtype groups. There was no statistical significance between the mean NOR count in the BAP1-mutant versus BAP1-wildtype groups ($P = 0.24$).

Custom Thresholding Method: The BAP1-mutant had a mean largest NOR pixel area of 47.62 (range 11 - 99) and a mean NOR count of 1.61 (range 1 - 8). The BAP1 wildtype group had a mean largest NOR pixel area of 47.38 (range 11 - 99) and a mean NOR count of 1.93 (range 1 - 9). There was no statistical difference between the mean pixel area of BAP1 mutant versus BAP1 wildtype ($P = 0.72$). A strong statistical significance was observed between the mean NOR count in the BAP1 mutant versus BAP1 wildtype groups ($P = 6.76E^{-24}$).

Conclusions

The manual measurement method demonstrated that BAP1-mutant UMs tend to have larger nucleoli and fewer NORs than BAP1-wildtype UMs. This finding supports previous research regarding the prognostic relevance of nucleolar size and NOR number in high-risk versus low-risk UMs—alterations in BAP1 may account for these observations.

Given the three tested methodologies, the manual measurement method using Phillips Intellisite Suite outperformed both of the automated image analysis methods using two different thresholding techniques. Of these two techniques, the adaptive thresholding yielded more accurate pixel area measurements, whereas the custom thresholding yielded more accurate NOR counts.

Refinement of these image analytical techniques will be necessary for future studies. With incorporation of other known BAP1 associated morphometric parameters, use of advanced image analysis methods on digitally scanned H&E slides may allow for prediction of BAP1 status and GEP Class in UM.

References

1. Tr Am Acad Ophthalmol Otolaryngol. 1931;36:131–142.
2. Am J Ophthalmol. 1983 Oct;96(4):502-9. doi: 10.1016/s0002-9394(14)77914-0. PMID: 6624832.
3. Pathol Res Pract. 1989 Nov;185(5):631-4. doi: 10.1016/S0344-0338(89)80208-0. PMID: 2696944.
4. Cancer. 1997 Mar 1;79(5):982-8. PMID: 9041161.
5. Cancer Res. 2004 Oct 15;64(20):7205-9. doi: 10.1158/0008-5472.CAN-04-1750. PMID: 15492234; PMCID: PMC5407684.
6. Science. 2010 Dec 3;330(6009):1410-3. doi: 10.1126/science.1194472. Epub 2010 Nov 4. PMID: 21051595; PMCID: PMC3087380.
7. Transl Vis Sci Technol. 2019 May 6;8(3):11. doi: 10.1167/tvst.8.3.11. PMID: 31110912; PMCID: PMC6504204.
8. Exp Eye Res. 2020;193:107987. doi:10.1016/j.exer.2020.107987
9. Nat Methods. 2021 Jan;18(1):100-106. doi: 10.1038/s41592-020-01018-x. Epub 2020 Dec 14. PMID: 33318659.
10. PeerJ. 2014 Jun 19;2:e453. doi: 10.7717/peerj.453. PMID: 25024921; PMCID: PMC4081273.
11. Nat Methods. 2020 Mar;17(3):261-272. doi: 10.1038/s41592-019-0686-2. Epub 2020 Feb 3. Erratum in: Nat Methods. 2020 Feb 24;. PMID: 32015543; PMCID: PMC7056644.

Disclosures

This work was supported in part by California Institute for Regenerative Medicine CIRM DISC2-10973, VA Merit I01BX002284 and VA Merit I01RX002340, from the United States (U.S.) Department of Veterans Affairs Biomedical Laboratory Research and Development Service and the Rehabilitation Research and Development Service.